We are IntechOpen,
the world's leading publisher of
Open Access books
Built by scientists, for scientists

4,800
Open access books available

122,000
International authors and editors

135M
Downloads

Our authors are among the

154
Countries delivered to

TOP 1%
most cited scientists

12.2%
Contributors from top 500 universities

BOOK
CITATION
INDEX
CLARIVATE ANALYTICS
INDEXED

WEB OF SCIENCE™

Selection of our books indexed in the Book Citation Index
in Web of Science™ Core Collection (BKCI)

Interested in publishing with us?
Contact book.department@intechopen.com

Numbers displayed above are based on latest data collected.
For more information visit www.intechopen.com

Optical Beam Steering
using a 2D MEMS Scanner

Yves Pétremand[1], Pierre-André Clerc[1], Marc Epitaux[2], Ralf Hauffe[3],
Wilfried Noell[1] and N.F. de Rooij[1]
[1]Ecole Polytechnique Fédérale de Lausanne (EPFL)
[2]formerly at Intel Corporation, Newark, CA
[3]Hymite GmbH, Berlin
[1]Switzerland
[2]USA
[3]Germany

1. Introduction

Being currently performed on highly complex and expensive equipments, active optical alignment of single mode 10 Gb/s transmitters and receivers is proving to be the bottleneck process for high volume manufacturing (epitaux2005). In order to alleviate this production burden, new integrated technologies are required to align micro-components like micro-lenses and optical fibers with photonic devices. Although passive alignment using Silicon micro-machined V-grooves seems to be very attractive at first, it has only been successfully implemented for micro-lens which can tolerate up to several microns of misalignment (osenbach1998). Alternative solutions such as active MEMS alignment techniques have been employed mainly for switching applications. They are based on actuated micro-mirrors, causing incident collimated beams to be reflected onto another mirror or a focusing lens to illuminate a waveguide (syms2002, pezeshki2002). A feedback loop mechanism is usually employed to dynamically optimize the coupling. Mostly used to select optical channels, these micro-mirror active alignment methods require complicated collimator and pigtail configurations and lack the possibility of locking them at the optimal position.

To resolve the latter issue, we propose a MEMS XY scanner mounted with a micro-lens to actively perform optical alignment of fiber optics modules by steering a beam. Although similar techniques have been demonstrated (toshiyoshi2003, sunghoon2002), we describe a unique technology using a 2x2.7 mm silicon bulk micro-machining chip characterized by ±30 µm XY range of motion (petremand2004), electrostatic comb drives actuation and a silicon hybrid lens with alignment locking capability.

Presently, transceivers are mainly assembled into TO can systems (epitaux2005b, petremand2005). In the described work, the MEMS device is dedicated to be assembled into a vertical silicon optical bench. In this system, the beam propagates vertically through a stack of micro-machined silicon devices which comprise substrate, RF feed-through, hermetic sealing and optical alignment functions.

This chapter will first present the system concept and the MEMS device. Secondly, design and simulations performed with CoventorWare and CoventorWare-Architect will be shown. Thirdly, the fabrication process will be presented. Finally, the packaging technology will be explained and characterization results of the fabricated MEMS device as well as a fully assembled and functional system will be discussed.

2. Scanner design

Fig. 1 shows the concept of the described application of the MEMS device. By placing a lens on the 2D movable platform of the actuator, it is possible to steer the light beam coming out of the laser diode and couple it into a single mode fiber. Working in the infrared region of the spectrum (wavelength usually used in telecommunications), all the MEMS components can be micro-machined out of silicon.
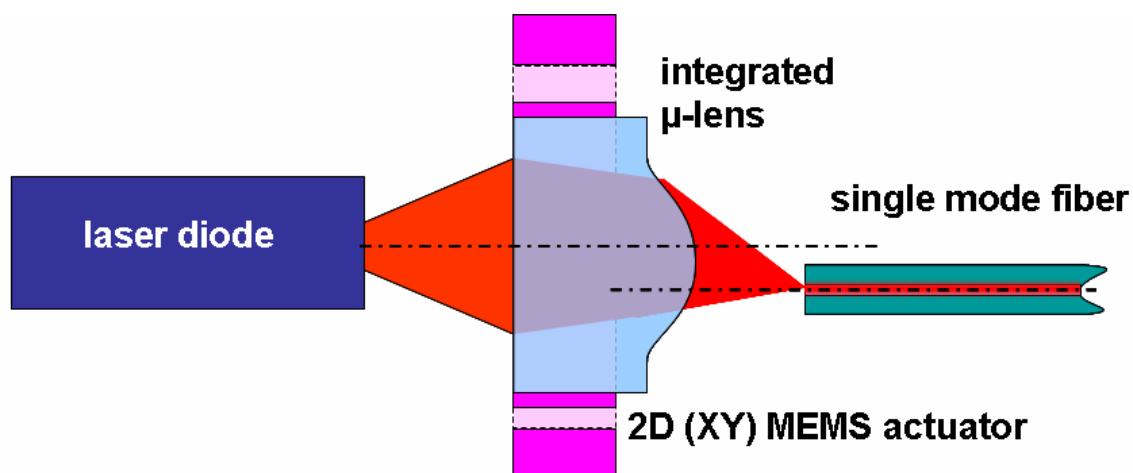

Fig. 1. Optical scheme of the light coupling concept.

Due to fabrication costs and available technology, it was chosen to assemble the silicon lens on top of the platform instead of integrating it directly on the MEMS. The advantages of such an assembly are the following:

- The cost of the device is reduced as one can manufacture more microlenses per surface unit by using a dedicated wafer.
- The cost of effective anti-reflecting coating on the lenses is reduced and facilitated.
- The technology is simplified as there is no need to protect the microlens during the HF release step of the process.

The principle of operation of the micromachined scanner is shown in Fig. 2. The 2D displacement of the hollowed platform of the device is provided by two pairs of electrostatic combdrive actuators (A, B, C and D, see Fig. 3) suspended by 4 springs to the chip base (petremand2004). The mobile platform is linked to the actuators by 4 compliant curved beams. These flexible arched beams are designed to convert two unidirectional (X) actuations into two dimensional (XY) displacements and as well as to amplify the movement in the direction orthogonal to the actuators by a factor of two. When the two actuators are moving accordingly by the same orientation and amount, the platform translates in the same orientation and by the same distance (displacement in X). Additionally when the two actuators are moving in opposite directions by the same amount, the platform translates in
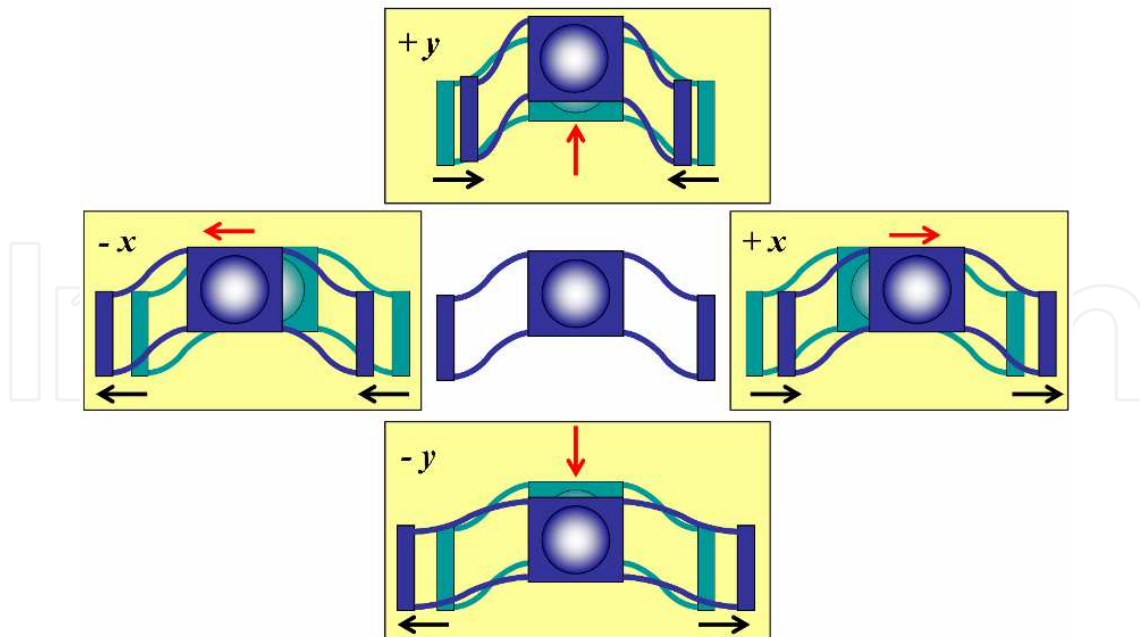
Fig. 2. Principle of operation of the MEMS scanner. By combining these basic displacements, any point of the scanning area can be reached.
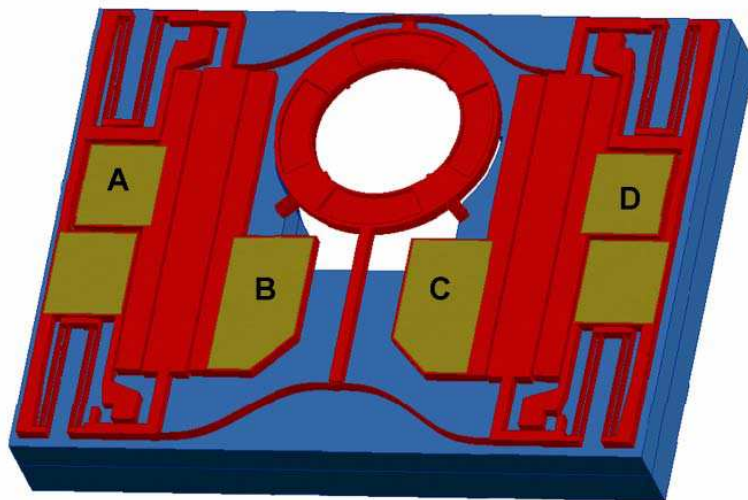

Fig. 3. CAD image of the device showing the two pairs of electrostatic combdrive actuators, the compliant suspension springs and the movable platform.

the orthogonal direction by either compressing or extending the compliant beams (displacement in Y). Fig. 2 shows the displacements along the two main axes (X) and (Y). With combining these basic displacements by applying different signal amplitudes to combdrive actuators, any off-axis points of the reachable area can be addressed.

Once the desired position reached, the movable platform can be locked in place by applying a voltage between the movable platform and the base of the chip (Fig. 4). Depending on the electrical current and the voltage applied, the locking is either temporary or permanent. In case of a temporary locking, the platform is held in place as long as the licking voltage is applied. For the permanent one, the platform stays at the desired position even after all the voltages are set back to zero.

The backside of the chip includes a through hole under the platform to accommodate the movable lens and transmit light across the MEMS chip.
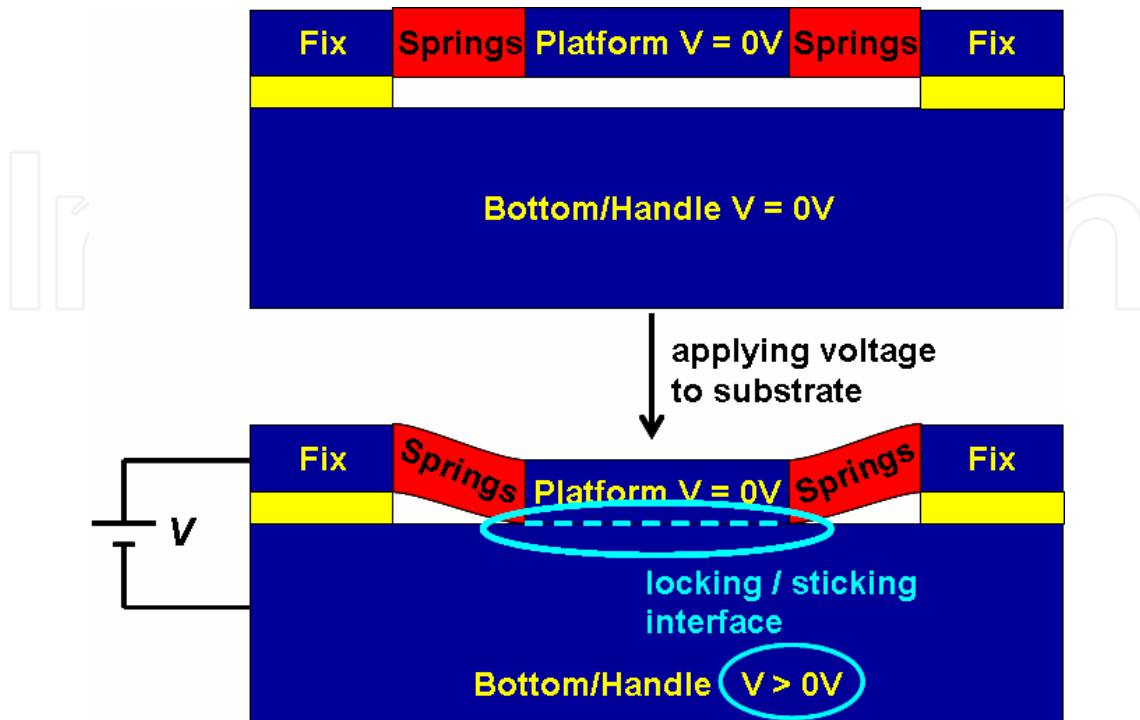

Fig. 4. Locking mechanism principle. Device layer is pulled down to the handle by applying a voltage between these two layers. Depending on the voltage/current applied, the resulting locking mechanism can be either temporary or permanent.

3. Simulations

Simulations were carried out to optimize the size and the shape of the compliant beams. By comparing straight and curved beams, for a given deformation, the maximal stress occurs in the same region of the beam but its value is different. In case of a straight beam, a maximal stress of 160 MPa was obtained while the maximal stress of the curved beam was 110 MPa. The curved beam shape allows a reduction of the maximal stress of more than 30%, which is very positive as the stress can be the cause of fatigue or breakage of the device.
In order to obtain a large enough scanning range in the Y direction even if the system is moved in the X direction, as the total displacement of the combdrives is limited, the shape of the curved springs was optimized to amplify the Y displacement with a factor of two. That way, if both actuators are displaced of a distance x in opposite directions, the corresponding perpendicular motion y of the platform is the following:

$$y \cong 2x \tag{1}$$

This result was obtained with a beam given by the following equation (karthe1991):

$$y(x) = \frac{\sqrt{2}}{4}x - \frac{\sqrt{2}L}{8\pi}\sin\left(\frac{2\pi}{L}x\right) \tag{2}$$

where L is the length of the beam.

Fig. 5 shows a schematic of the movement of the beam as force is applied on the movable end. Architect simulations results are shown in Fig. 6. For these simulations, a beam slightly simplified was used. In Architect, a model exists for the simulation of "freeform beams". These can be defined either by a polynomial equation or by points. The approximation of the shape described in equation 2 was performed with a set of 13 coordinates.
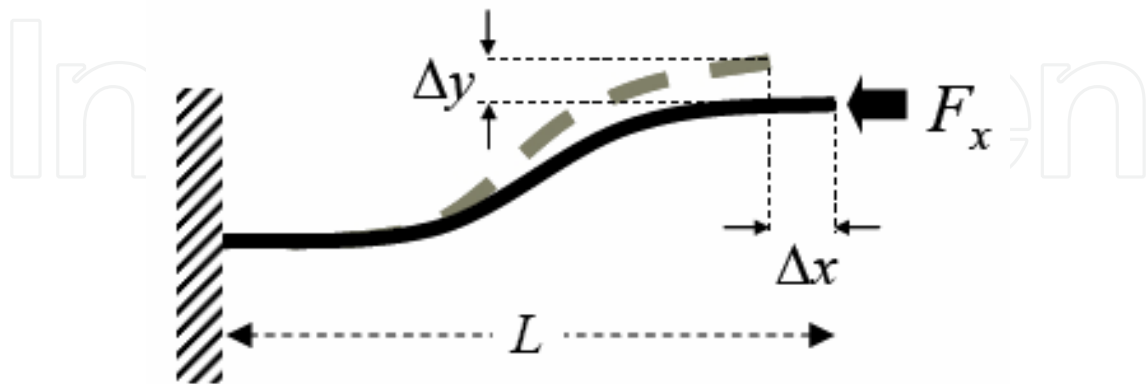

Fig. 5. Schematic view of the movement of the free end of the compliant curved beam as a force is applied to.
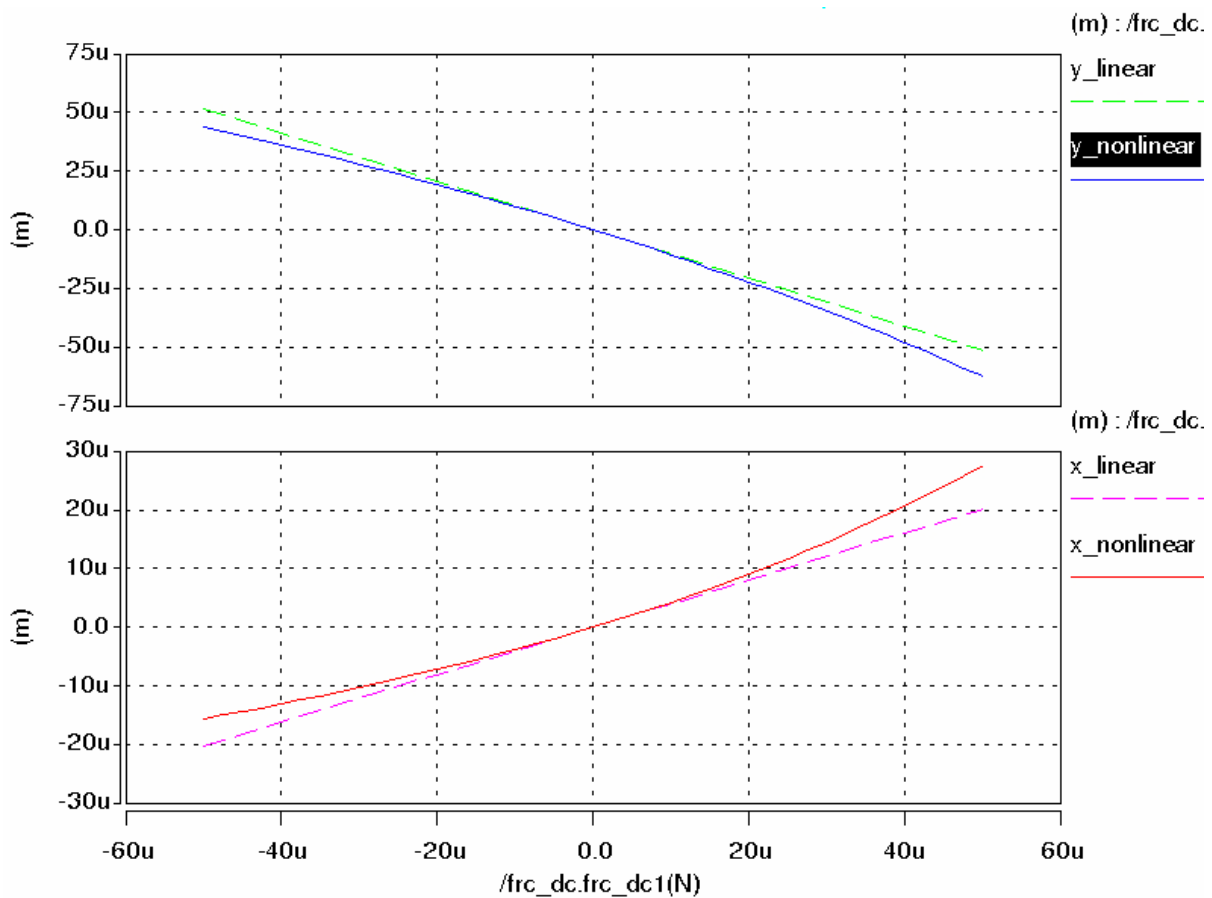
Fig. 6. Architect results of the simulation of the curved beam. In each graph, the linear and non-linear simulation modes are represented. The top image represents the displacement along the Y axis (Δy on Fig. 5) and the bottom one represents the displacement along the X axis (Δx on Fig. 5).

With such spring shape, one obtains the displacements of the platform shown on Fig. 7. This simulation visualizes the result of the shape of the beams but not their width. By changing the beam width, same behavior of the device was obtained but at different voltages.
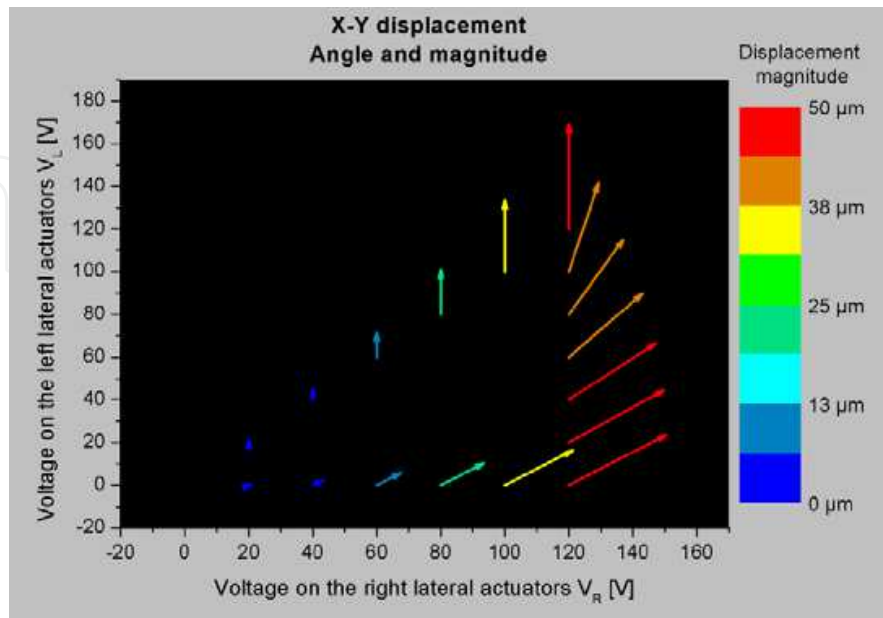

Fig. 7. Coventor simulation showing the displacement of the central platform in respect to voltages applied on two combdrives. This graph corresponds to one quarter of the total area reachable of the platform.

4. Fabrication process

For the fabrication four main process steps are performed: oxidation, metallization, DRIE with a delay mask process and etching of the sacrificial oxide layer. In between, to pattern the different layers, photolithographic steps have to be completed.

After metallization, PECVD oxide deposition is performed to avoid any contamination of gold during the rest of the process. As gold is known to be highly contaminant, it has to be buried in order not to expose the equipment used later in the process.

One challenge of this process is to perform a double bulk micromachining delay mask process. On the device layer side, shallow cavities are etched to allow the assembly of the lens on top of the MEMS. On the handle layer, deep openings on two levels had to be performed in order to create a cavity where the laser diode will be placed into.

The chips are finally released and singulated using HF vapor phase etching.

5. Packaging technology

The packaging technology approach is depicted in Fig. 8. The configuration is similar to a TO-can package with a coaxial optical connector. The TO header is replaced by a vertical hermetic Silicon Bench sub-assembly. In contrast to TO package assembly, the receptacle is simply passively bonded to this sub-assembly without requiring complex active alignment and welding equipment. The silicon sub-assembly is further illustrated in Fig. 8 b). It consists of a system composed of two micromachined silicon layers and a silicon microlens.

The first chip carries the active optical elements such as the laser diode, monitoring photodiode and other miscellaneous electrical components. As an edge emitting laser is used, a turning mirror is placed on the substrate to deflect the laser beam towards the other silicon sayers and the connector. The 2D MEMS scanner with the pre-mounted lens is assembled on top of the laser diode and the turning mirror. It is electrically connected to the first layer by wire bonding. This silicon sub-assembly is then hermetically sealed with a glass lid and flip-chip bonded on a flexprint containing the contacts to connect the system to the external elements.

(a)   (b)
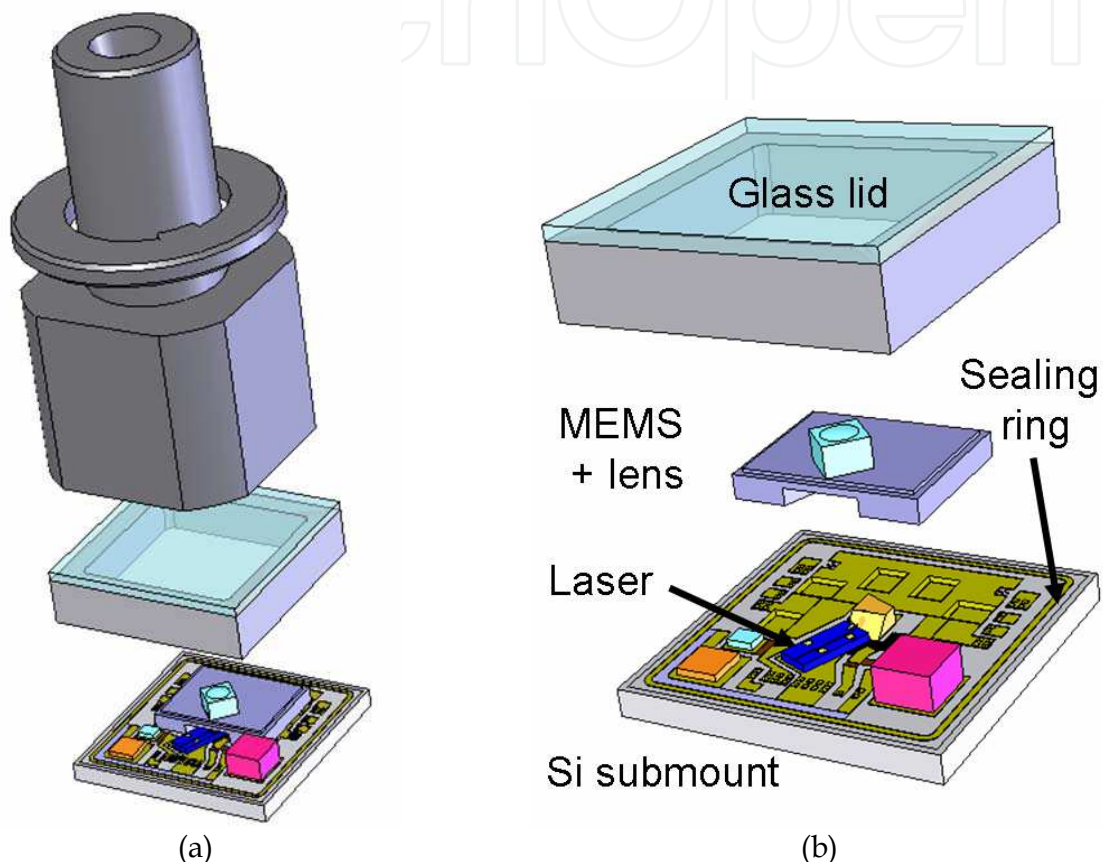
Fig. 8. Model of the system based on Vertical Optical Bench. a) General view of the packaging with the device module and the fiber ferrule. b) Detailed view of the device module with the glass lid, the silicon chip, the silicon submount containing the laser diode, the turning mirror and electronic components. The MEMS chip is partially hollowed out on the backside to allow space for the laser diode and turning mirror.

6. Experimental results

Fig. 9 shows a SEM image of the fabricated device with the silicon lens assembled on top of the movable platform. The bright parts of the image correspond to the metal pads defined to be connected by wire bonding.

Displacements of the platform were performed by applying voltages on the electrodes of the chips. Fig. 10 shows the maximal displacements achieved with a device with springs and compliant beams width designed at 3.5 µm. Depending on the width of the springs, the displacements obtained are the same but correspond to excitations with different amplitudes.
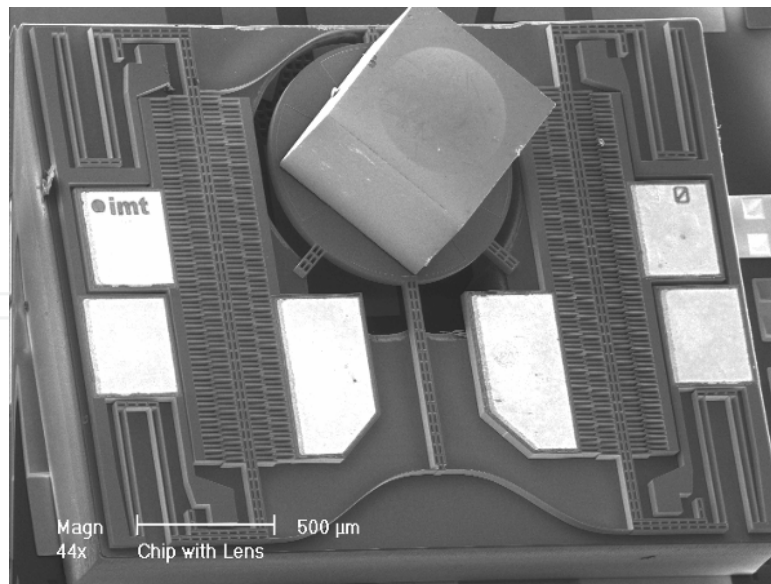
Fig. 9. MEMS device with a silicon lens assembled on top. This sub-assembly will be positioned on a submount over a laser diode (Fig. 8 b).
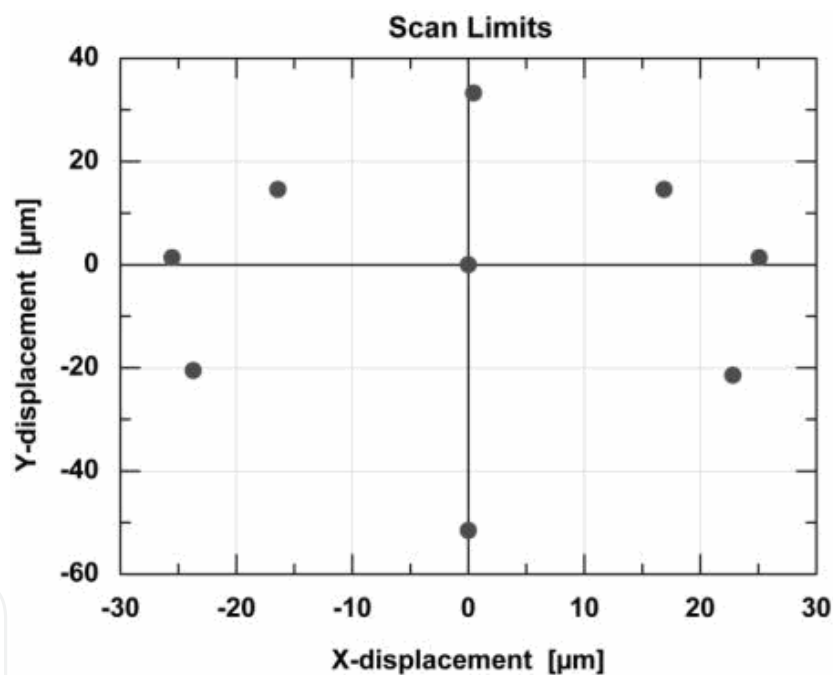

Fig. 10. Maximal displacements achieved with the scanning platform.

Resonance frequency was measured and compared to simulated values. Fig. 11 shows the resonance frequency calculated from the step response measurements performed with a Wyko DMEMS white light interferometer. It was performed by applying a Fourier transform (Fig. 11 b)) to the step response of the actuator (Fig. 11 a)). It gives a resonance frequency of 717.2 Hz. This measurement was carried out on a chip before assembly and packaging (i.e. without lens). This value can be compared to the simulated value shown in Fig. 12 where the resonance frequency was 698.83 Hz. These results are in very good agreement, the error between the measured and the simulated value being less than three percent.

Although the frequency values are very close, it is not the case of the damping coefficients. It can be seen on (Fig. 11 a)) that the measured damping value is very low. It is much lower than the simulated one. These differences are not understood yet and have to be further investigated.
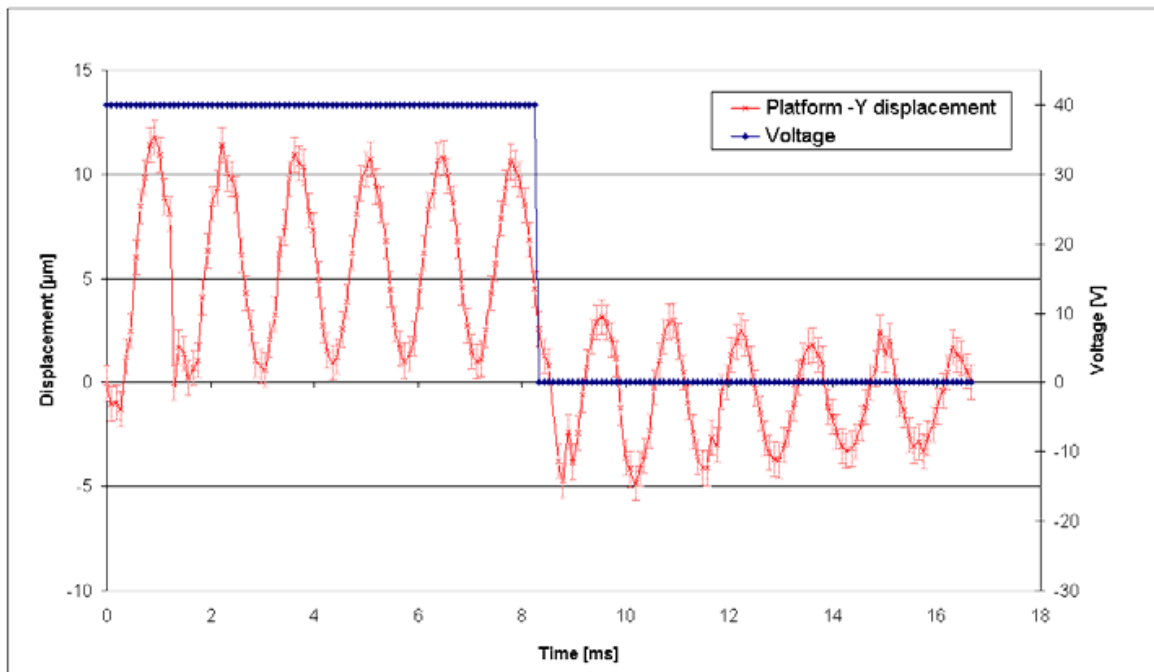
a)
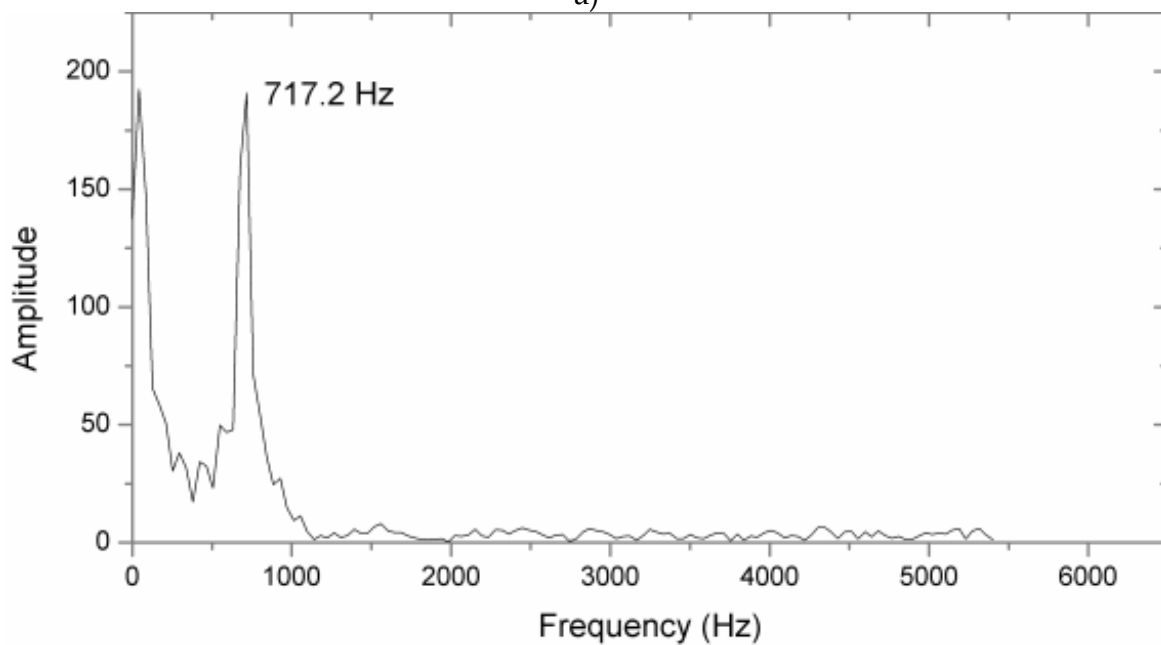
b)

Fig. 11. Determination of the resonance frequency by measuring the step response in "-Y" direction (Fig. 2) of a fabricated actuator. a) Measured displacement of the actuator and voltage applied on the combdrives. b) Fourier transform of the obtained step response.

The assembly of a complete system was then carried out (Fig. 13) and optical measurements of beam steering were performed. A complete assembly process flow had to be developed to assemble the different components of the system. Fig. 13 a) shows this procedure. First subassemblies are performed to glue the lens on the MEMS device and to bond the electronic components including the laser diode on the submount. Both are then assembled, wire bonded and protected by a cover glass. The measured and simulated displacements of the platform and the beam steering measurement angle were compared. By plotting the optical measurements and the simulations performed previously in the same graph, a good agreement of both (normalized) data sets can be observed (Fig. 14).
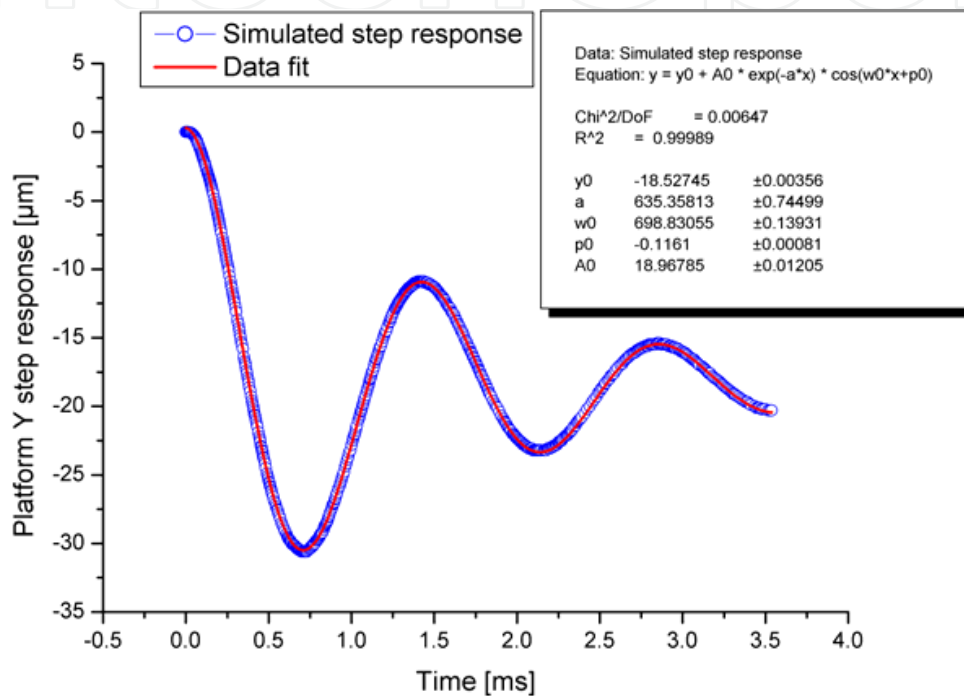

Fig. 12. Simulation of the step response of the actuator in "-Y" direction (Fig. 2). The fitted curve shows a frequency of 698.83 Hz. Excellent agreements between the simulated and the measured values (Fig. 11).

7. Conclusion

A bi-directional MEMS-based optical beam steerer was fabricated and assembled. The assembly of the different parts of the system was carried out. A displacement of several tens of micrometers has been demonstrated and optical beamsteering was shown with a system containing all the electronic and optical components. Resonance frequency and displacements measurements agree with the simulated ones. This displacement range is suitable for opto-electronic alignment applications.

8. Acknowledgments
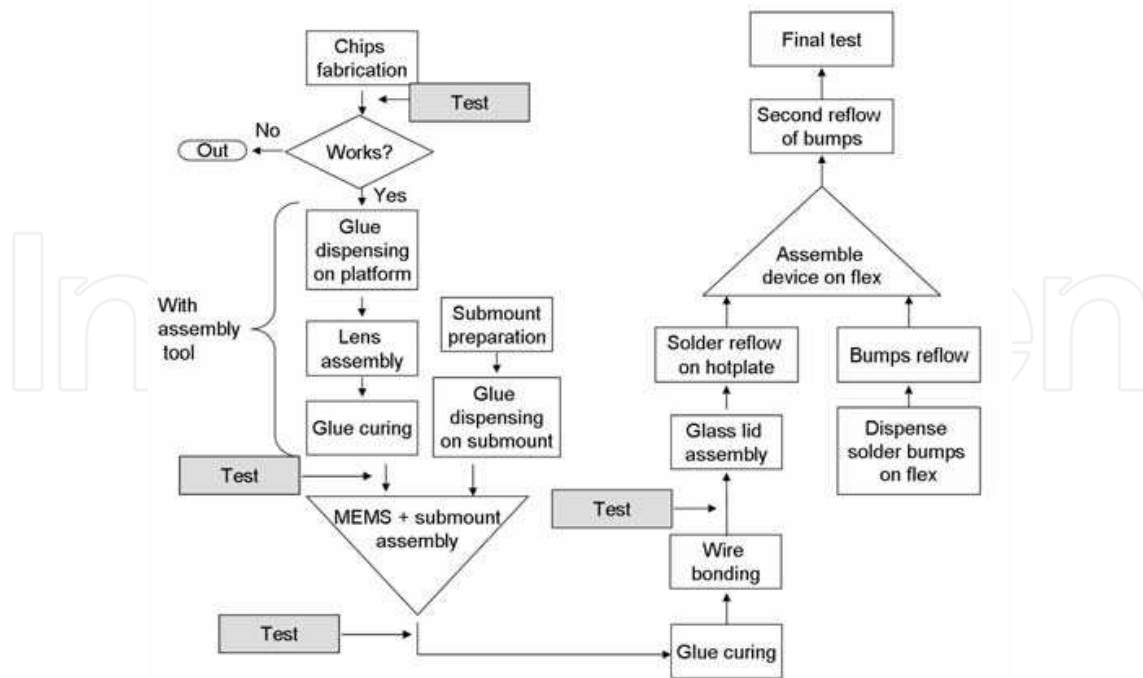
a)

b)

Fig. 13. Assembly of the MEMS device. a) Flowchart of the assembly process. b) Fully assembled system comprising flexprint, MEMS, microlens, electronic components, laser diode and glass lid.
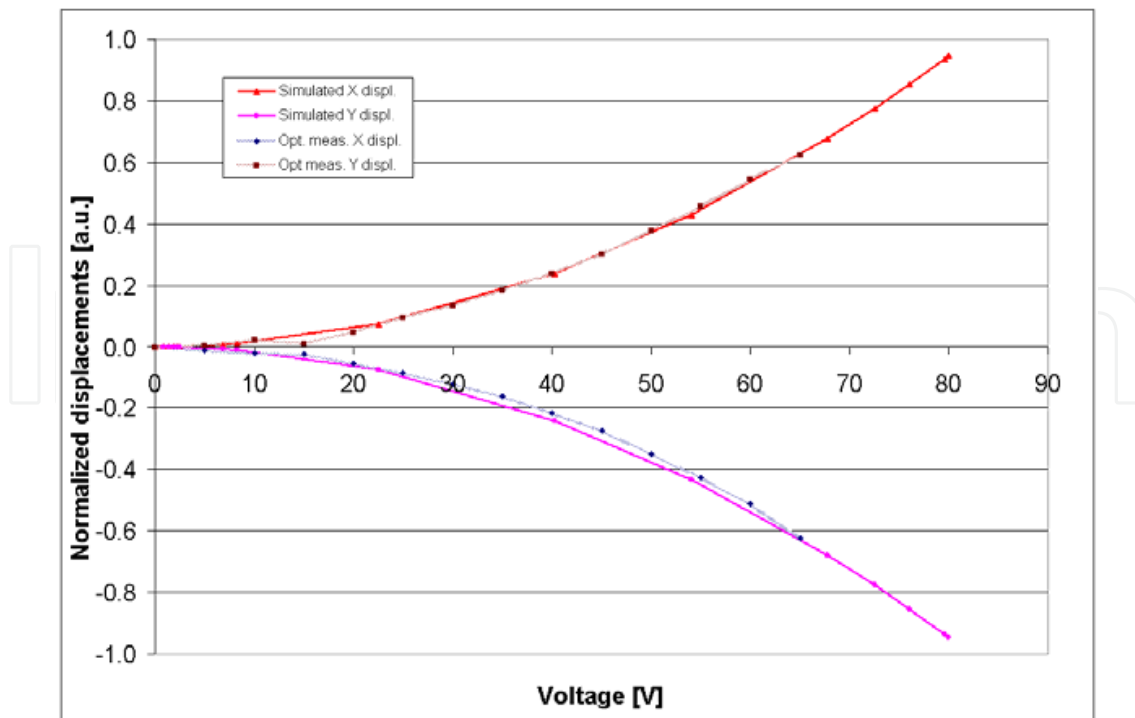
Fig. 14. Comparison between the simulated and optically measured data (both normalized). Both X and Y measured trajectory curves are very close to the simulated ones.

9. References

epitaux2005, M. Epitaux, Y. Pétremand, W. Noell, N.F. de Rooijand J.-M. Verdiell,. (2005). Silicon Optical Benches for Next Generation Optical Packaging: Going Vertical or Horizontal?, *in IEEE 2005 Electronic Components and Technology Conference*, 2005, volume 2, pages 1339-1342

osenbach1998, J.W. Osenbach et al. (1998). Low colt/high volume laser modiles using silicon optical bench technology, *in Electronic Components and Technology Conference*, 1998, pages 581-587

syms2002, Richard R.A. Syms and D.F. Moore. (2002). Optical MEMS for Telecom, *in Materials today*, 2002, pages 26-35

pezeshki2002, B. Pezeshki et al. (2002). 20-mW Widely Tunable Laser Module Using DFB Array and MEMS Selection, *in IEEE Photonics Technology Letters*, volume 14, pages 1457-1459

toshiyoshi2003, H. Toshiyoshi, G.-D. J. Su, J. LaCosse and M. C. Wu. (2003) Surface Micromachined 2D Lens Scanner Array, *in IEEE Optical MEMS Conference 2003,*

sunghoon2002, K. Sunghoon and L.P. Lee. (2002). Stacked Two Dimensional Micro-Lens Scanner for Micro Confocal Imaging Array, *in IEEE Micro Electro Mechanical Systems Conference 2002*, pages 483-486

petremand2004, Y. Pétremand et al. (2004). Novel 2D MEMS based Optical Beamsteerer, *in IEEE Optical MEMS 2004*, pages 58-59

epitaux2005b, M. Epitaux et al. (2005). Micro-Machined XY Stage for Fiber Optics Module Alignment, *in IEEE Optical Fiber Communications Conference Technical Digest 2005*

petremand2005, Y. Pétremand et al. (2005) Post assembly alignment system, *in 10th International Commercialization of Micro and Nano Systems Conference 2005*, pages 477-481

karthe1991, W. Karthe and R. Müller. (1991). *INTEGRIERTE OPTIK*, Akademische Verlagsgesellschaft Geest & Portig, ISBN 3321000806, 9783321000805
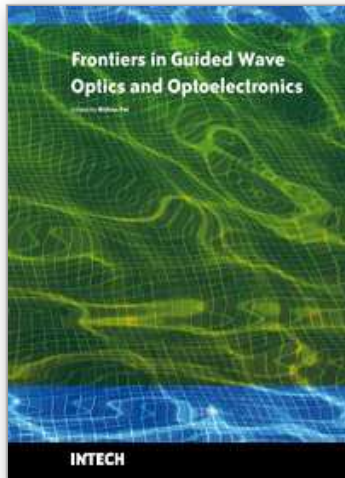
Frontiers in Guided Wave Optics and Optoelectronics

Edited by Bishnu Pal

ISBN 978-953-7619-82-4

Hard cover, 674 pages

Publisher InTech

Published online 01, February, 2010

Published in print edition February, 2010

As the editor, I feel extremely happy to present to the readers such a rich collection of chapters authored/co-authored by a large number of experts from around the world covering the broad field of guided wave optics and optoelectronics. Most of the chapters are state-of-the-art on respective topics or areas that are emerging. Several authors narrated technological challenges in a lucid manner, which was possible because of individual expertise of the authors in their own subject specialties. I have no doubt that this book will be useful to graduate students, teachers, researchers, and practicing engineers and technologists and that they would love to have it on their book shelves for ready reference at any time.

How to reference

In order to correctly reference this scholarly work, feel free to copy and paste the following:

Yves Pétremand, Pierre-André Clerc, Marc Epitaux, Ralf Hauffe, Wilfried Noell and N.F. de Rooij (2010). Optical Beam Steering Using a 2D MEMS Scanner, Frontiers in Guided Wave Optics and Optoelectronics, Bishnu Pal (Ed.), ISBN: 978-953-7619-82-4, InTech, Available from: http://www.intechopen.com/books/frontiers-in-guided-wave-optics-and-optoelectronics/optical-beam-steering-using-a-2d-mems-scanner

INTECH
open science | open minds